Hydrogen concentration behavior of y - grooved weld joint based on a coupled analysis of heat transfer - thermal stress - hydrogen diffusion

Go Ozeki[1*], A. Toshimitsu Yokobori, Jr.[1], Toshihito Ohmi[2], Tadashi Kasuya[3], Nobuyuki Ishikawa[4], Satoshi Minamoto[5], Manabu Enoki[3]

[1]Strategic Innovation and Research Center, Teikyo University, Tokyo, 173-8605, Japan
[2]Department of Mechanical Engineering, Shonan Institute of Technology, Kanagawa, 251-8511, Japan
[3]Graduate School of Engineering, The University of Tokyo, Tokyo, 113-8656, Japan
[4]Steel Research Laboratory, JFE Steel Corporation, Kanagawa, 210-8555, Japan
[5]Research and Services Division of Materials Data and Integrated System, National Institute for Materials Science, Ibaraki, 305-0047, Japan

*Corresponding author

DOI: 10.5185/amlett.2018.2160
www.vbripress.com/aml

Abstract

It is important to predict the stress driven hydrogen induced cracking at the weld joint on the basis of computational mechanics from the view point of engineering problem. In this study, On the basis of proposed numerical analysis, behaviors of hydrogen diffusion and concentration during cooling process of y-grooved weld joint were analyzed and the mechanism of hydrogen induced cracking was investigated. One of authors has been proposed α multiplication method which magnifies the hydrogen driving term in the diffusion equation to realize correctly hydrogen concentration behaviors. In this study, the behaviors of hydrogen diffusion and concentration for the model of y-grooved weld joint was analyzed by combining α multiplication method with the coupled analyses of heat transfer – thermal stress – hydrogen diffusion. As a result, hydrogen was found to diffuse from weld metal to base metal through HAZ (Heat Affected Zone), and concentrate at the position of blunt angle side of weld groove bottom. It was found that hydrogen concentrates at the position of the local maximum value of hydrostatic stress gradient. This analytical result was found to well predict the actual hydrogen induced cracking of the y-grooved weld joint. Using this method of analysis, prediction of hydrogen induced cracking becomes possible.

Keywords: Hydrogen diffusion, heat transfer, thermal stress, coupled analysis, y-grooved weld joint.

Introduction

In terms of the reliability of the structure, cold cracking at the weld joint is a critical problem. Cold cracking occurs after the weld part was cooled. And, cold cracking is caused by hydrogen introduced into weld metal during welding [1]. Therefore, it is necessary to be clarified hydrogen diffusion and concentration behaviors at the weld joint. However, it is very difficult to observe the behavior of hydrogen diffusion experimentally. Hence, from the view point of engineering, the prediction of hydrogen diffusion and concentration behaviors based on numerical analysis is necessary. Especially, in the analysis of the welding part during the cooling process, it is important to perform the analysis taken into account for the time sequential change of physical properties such as diffusion coefficient and yield stress due to the temperature change.

In order to predict the hydrogen diffusion and concentration behaviors in metals, analytical treatment on the equation of hydrogen diffusion has been performed since 1970's [2-7]. Sofronis et al. analyzed the hydrogen diffusion behavior using the hydrogen diffusion equation considering the stress driving term under existence of diffusive and trapped hydrogen conditions [8]. However, this analysis is conducted to clarify the delayed fracture under an almost steady state condition [8]. Therefore, for the case of remarkable time sequential change of temperature and thermal stress such as during the cooling of weld metal, time sequential transition behaviors of hydrogen diffusion and concentration should be noticed. On the other hand, Yokobori et al. has proposed α multiplication method which magnifies stress driven term in the diffusion equation. This method enables us to realize the effect of local stress driven term on hydrogen diffusion [9, 10]. Additionally, for the application of actual engineering structure, the FEM (Finite Element Method)-FDM (Finite Difference Method) analytical method was proposed [9,11]. In this method, stress analysis is

conducted by FEM and diffusion analysis is conducted by FDM, respectively. Furthermore, by combining α multiplication method with the FEM-FDM method [9], not only hydrogen but also vacancy diffusion behavior induced by local stress field has been analyzed [9,11-12]. In order to analyze the hydrogen diffusion and concentration behaviors at the weld joint during cooling process, it is necessary to combine the analysis of heat transfer and thermal stress with hydrogen diffusion. However, there are not so many researches which performed the coupled analysis [13].

In this study, in order to clarify the behaviors of hydrogen diffusion and concentration during cooling process, coupled analyses of heat transfer – thermal stress – hydrogen diffusion combining with α multiplication method was conducted for the model of y-grooved weld joint.

Nomenclature

l_0	Length of analytical model
C	Hydrogen concentration
C_0	Hydrogen concentration in atmosphere
D	Diffusion coefficient ($= D_0 \exp(-Q/RT)$)
D_0	Diffusion constant independent of temperature
T	Absolute temperature
T_{out}	Temperature in atmosphere
Q	Activation energy of hydrogen diffusion
R	Gas constant
ΔV	Volume change due to accommodation of a hydrogen
σ_p	Hydrostatic stress
E	Young's modulus
ν	Poisson's ratio
σ_{ys}	Yield stress
$\overline{\sigma}$	Equivalent stress
H_p	Work hardening coefficient
$\overline{\varepsilon_p}$	Equivalent plastic strain
c_1, α^*, m_1	Constants
h	Hydrogen transfer coefficient
t_c	Time of hydrogen diffusion
t_h	Time of heat transfer
ρ	Density
c	Specific heat
k	Heat conductivity ($= \rho \cdot c \cdot a$)
a	Thermal diffusion coefficient
H	Surface coefficient of heat transfer
h_T	$=H/k$
$T\alpha$	Thermal expansion coefficient

Coupled analysis of heat transfer – Thermal stress – Hydrogen diffusion

In order to analyze the hydrogen diffusion and concentration behaviors at the weld joint during cooling process, coupled analysis of Heat transfer-Thermal stress-Hydrogen diffusion was developed. However, this analytical method used for this analysis is the same as the previous articles [13, 14], this is reshown as follows. At first, analysis of heat transfer was conducted by FDM. And, temperature at each grid obtained by heat transfer analysis was interpolated to each node for thermal stress analysis by FEM. Then, thermal stress was calculated for each node point using the interpolated temperature. After that, thermal stress obtained by this analysis was interpolated to each grid point for analysis of hydrogen diffusion by FDM. Using the interpolated thermal stress, stress driven hydrogen diffusion analysis was performed. By conducting sequentially these calculations mentioned above, hydrogen diffusion and concentration behaviors during cooling process were analyzed. The flowchart of this analysis is shown in **Fig. 1**.

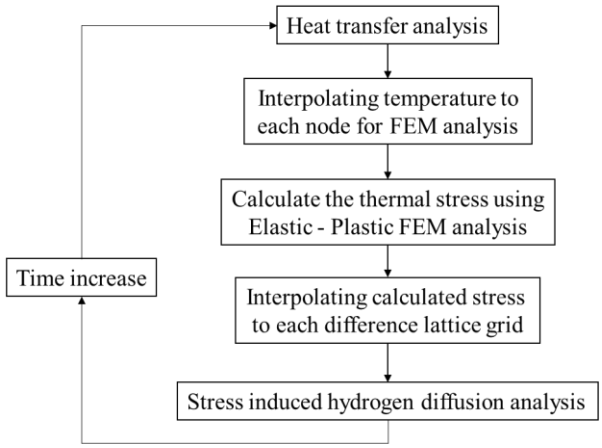

Fig. 1. Flowchart of coupled analysis of Heat transfer-Thermal stress-Hydrogen diffusion.

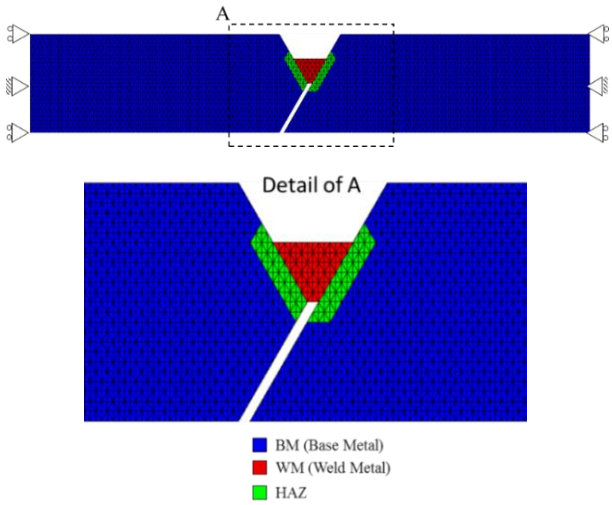

Fig. 2. Analytical model.

Analytical model and boundary conditions

In this study, y-grooved weld joint composed of WM (Weld Metal), HAZ (Heat Affected Zone) and BM (Base Metal) was designed on the basis of Japan Industrial Standards as shown in **Fig. 2** [15]. This analysis was performed as two-dimensional analysis. The number of nodes and elements are 6144 and 11713, respectively.

Table 1. Material properties for FEM analysis.

	E [GPa]	ν	σ_{ys} [MPa]	H_p [GPa]	$T\alpha$ [1/K]
WM	ref. [Fig. 3]	0.3	ref. [Fig. 4]	0.01× E	1.2E-05
HAZ					
BM					

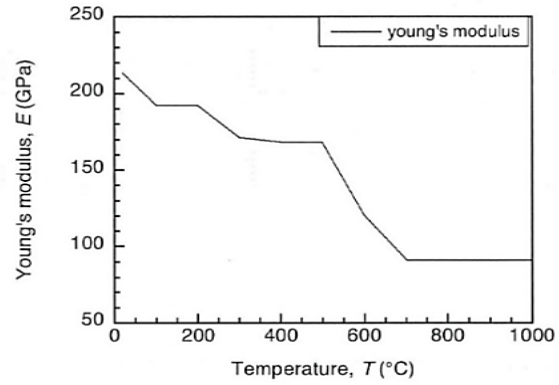

Fig. 3. Temperature dependence of Young's modulus [16].

The material properties used are shown in **Table 1**. Young's modulus and yield stress were changed depend on temperature as shown in **Fig. 3** and **Fig. 4** [16], respectively. Considering the cooling from high temperature, yield stress of martensitic structure shown in **Fig. 4** was used in this analysis [16]. For thermal expansion coefficient, the physical property of iron was used. And, this analysis was carried out under the conditions of eqn. (1) assuming that yield stress of WM and BM is lower than that of HAZ [17].

$$\sigma_{ys(WM,BM)} = 0.8\sigma_{ys(HAZ)}. \quad (1)$$

Young's modulus, Poisson's ratio and thermal expansion coefficient are the same for all elements regardless of difference of structure such as WM and HAZ. Values of work hardening coefficient were calculated by 0.01E as shown in **Table 1**. And, stress analysis was conducted under plane strain condition.

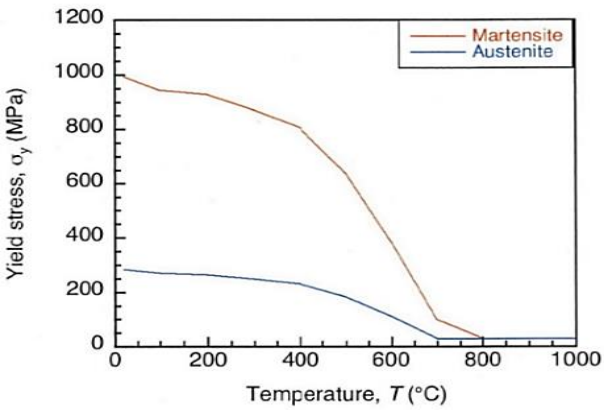

Fig. 4. Temperature dependence of yield stress[16].

Boundary conditions of heat transfer analysis and hydrogen diffusion analysis are shown in **Fig. 5.** The number of grid points for FDM is 1608.

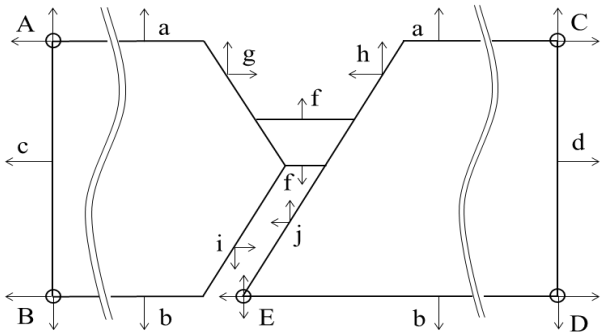

$$\frac{\partial C}{\partial x} = h(C - C_0),\ \frac{\partial T}{\partial x} = h_T(T - T_{out}) \ :\text{A, B, E, c, h, j}$$

$$\frac{\partial C}{\partial x} = h(C_0 - C),\ \frac{\partial T}{\partial x} = h_T(T_{out} - T) \ :\text{C, D, d, g, i}$$

$$\frac{\partial C}{\partial y} = h(C - C_0),\ \frac{\partial T}{\partial y} = h_T(T - T_{out}) \ :\text{B, D, b, f, i}$$

$$\frac{\partial C}{\partial y} = h(C_0 - C),\ \frac{\partial T}{\partial y} = h_T(T_{out} - T) \ :\text{A, C, a, f, g, h, j}$$

$$\frac{\partial C}{\partial y},\ \frac{\partial T}{\partial y} = 0 \ :\text{E}$$

Fig. 5. Boundary conditions of heat transfer and hydrogen diffusion analysis.

Heat transfer analysis

Heat transfer analysis was performed using eqn. (2).

$$\rho c \frac{\partial T}{\partial t_h} = k\left(\frac{\partial^2 T}{\partial x^2} + \frac{\partial^2 T}{\partial y^2}\right) \quad (2)$$

Eqn. (2) was discretized and solved by SOR (Successive-Over-Relaxation) method. This detailed method is mentioned in *Method of Numerical Analysis*.

Initial temperature at WM was 1500ºC, and at HAZ and BM were R.T.(20ºC). Boundary conditions for heat transfer analysis are shown in **Fig. 5**. Material properties used for heat transfer analysis are shown in **Table 2** [18]. Only cooling process from 1500ºC to R.T was considered for this analysis. And convection was not considered.

Table 2. Material properties used for heat transfer analysis[18].

k	0.054	J/(ºC·mm·sec)
a	12.0	mm^2/sec
$\rho \cdot c$	4.53×10^{-3}	J/(ºC·mm^3)
H	2.09×10^{-5}	J/(ºC·mm^2·sec)

Stress analysis

The routine of thermal stress analysis was added to the two-dimensional elastic-plastic FEM program EPIC-I [13-14,19]. The elastic plastic stress-strain law corresponding to the temperature change accompanied by heat transfer was also added to this program software. Therefore, the yielding and the plastic deformation characteristics were adjusted to the temperature change.

The elastic deformation is approximated by Hooke's law. And, the characteristic of work-hardening for plastic deformation H_p is approximated by eqn. (3).

$$H_p = \frac{d\bar{\sigma}}{d\bar{\varepsilon}_p} = m_1 c_1 \left(\alpha * + \bar{\varepsilon}_p\right)^{m_1 - 1} \quad (3)$$

In this analysis, linear work hardening law as $m_1 = 1$ was used.

Hydrogen diffusion analysis

The basic equation of hydrogen diffusion [3] is written as

$$\frac{\partial C}{\partial t_C} = \nabla\left(D\nabla C - DC\frac{\Delta V}{RT}\nabla\sigma_p\right) \quad (4)$$

The first and second terms are those of hydrogen diffusion due to the concentration gradient and due to the stress gradient, respectively. Value of the stress gradient term is usually lower order than that of the concentration gradient term. For such case, the effect of concentration gradient term on hydrogen diffusion appears alone and the effect of stress gradient term on hydrogen diffusion does not operate [9, 10]. Under this situation, it has been reported that the effect of local stress driven effect on hydrogen concentration given by the second term of eqn. (4) was found to appear by adding the weight coefficient to this term in eqn. (4) in order to take the same effect as that of the first term of eqn. (4) [9,10]. This method is proposed as the α multiplication method [9, 10]. By adding the weight coefficient to each term eqn. (4), eqn. (5) was obtained.

$$\frac{\partial C}{\partial t_C} = \alpha_1 D\nabla^2 C - \alpha_2 \frac{D\Delta V}{RT}\nabla C\nabla\sigma_p - \alpha_3 \frac{D\Delta V}{RT} C\nabla^2\sigma_p \quad (5)$$

In this study, in order to make the effect of concentration gradient and stress gradient are the same order, the weight coefficients $\alpha_{1\sim3}$ take $\alpha_1:\alpha_2:\alpha_3 = 1:1000:5$. And, as an initial condition, initial hydrogen concentration was assumed to be $C/C_0 = 3.0$ in the weld metal. In the other region, initial hydrogen concentration was $C/C_0 = 1.0$. The material properties used for hydrogen diffusion analysis are shown in **Table 3** [6,20].

Where the physical meaning of α is considered to be the ratio of the diffusion entropy differences due to the different driven potentials in the diffusion process by concentration gradient and stress gradient [21]. Therefore, α is the coefficient taken into account for the effect of difference of entropy on diffusion coefficient.

Table 3. Material properties used for Hydrogen diffusion analysis [6,20].

D_0	5.54×10^{-6}	m/sec
Q	26.81×10^{3}	J/mol
R	8.314	J/K mol
ΔV	2.0×10^{-6}	m^3/mol

Method of numerical analysis

In this analysis, the heat transfer and the diffusion equation shown in eqn. (2) and eqn. (5) were discretized using the Crank-Nicolson implicit method. And the simultaneous equations were solved by the SOR method for eqn. (2) and by SUR (Successive-Under-Relaxation) method for eqn. (5) [10]. The detailed method is as follows.

In order to eliminate the physical property on the basic equation and make general analysis, eqn. (2) and eqn. (5) were normalized using eqns. (6a) - (6d) and eqns. (7a) - (7e).

$$x^+ = \frac{x}{l_0}, \quad (6a)$$

$$y^+ = \frac{y}{l_0}, \quad (6b)$$

$$t_h^+ = \frac{at_h}{l_0^2}, \quad (6c)$$

$$a = \frac{k}{\rho c}. \quad (6d)$$

$$x^+ = \frac{x}{l_0}, \quad (7a)$$

$$y^+ = \frac{y}{l_0}, \quad (7b)$$

$$C^+ = \frac{C}{C_0}, \quad (7c)$$

$$D^+ = \frac{D}{D_0}, \quad (7d)$$

$$t_C^+ = \frac{t_C D_0}{l_0^2}. \quad (7e)$$

As a result, eqn. (8) and eqn. (9) were obtained.

$$\frac{\partial T}{\partial t_h^+} = \left(\frac{\partial^2 T}{\partial x^{+2}} + \frac{\partial^2 T}{\partial y^{+2}}\right), \quad (8)$$

$$\begin{aligned}\frac{\partial C^+}{\partial t_C^+} = \alpha_1 \Bigg\{ & D^+\left(\frac{\partial^2 C^+}{\partial x^{+2}} + \frac{\partial^2 C^+}{\partial y^{+2}}\right) \\ & + \left(\frac{\partial D^+}{\partial x^+}\frac{\partial C^+}{\partial x^+} + \frac{\partial D^+}{\partial y^+}\frac{\partial C^+}{\partial y^+}\right)\Bigg\} \\ & - \frac{\Delta V}{R}\Bigg[\alpha_2\Bigg\{\frac{C^+}{T}\left(\frac{\partial D^+}{\partial x^+}\frac{\partial \sigma_p}{\partial x^+} + \frac{\partial D^+}{\partial y^+}\frac{\partial \sigma_p}{\partial y^+}\right) \\ & + \frac{D^+}{T}\left(\frac{\partial C^+}{\partial x^+}\frac{\partial \sigma_p}{\partial x^+} + \frac{\partial C^+}{\partial y^+}\frac{\partial \sigma_p}{\partial y^+}\right) \\ & - \frac{D^+ C^+}{T^2}\left(\frac{\partial T^+}{\partial x^+}\frac{\partial \sigma_p}{\partial x^+} + \frac{\partial T^+}{\partial y^+}\frac{\partial \sigma_p}{\partial y^+}\right)\Bigg\} \\ & + \alpha_3 \frac{D^+ C^+}{T}\left(\frac{\partial^2 \sigma_p}{\partial x^{+2}} + \frac{\partial^2 \sigma_p}{\partial y^{+2}}\right)\Bigg].\end{aligned} \quad (9)$$

In hydrogen diffusion equation, ∇D, ∇C and $\nabla \sigma_p$ are included as shown in eqn. (9). Therefore, hydrogen diffusion and concentration behaviors depend on the gradient of diffusion coefficient, hydrogen concentration and stress. Then, eqn. (8) and eqn. (9) were discretized using Crank-Nicolson implicit method. And, by coordinating the left hand side as unknown term (time step n+1) and the right hand side as known term (time step n), eqn. (10) and eqn. (12) were obtained, respectively.

$$\begin{aligned}&\left(1+r_x+r_y\right)T_{i,j,n+1}-\frac{r_x}{2}T_{i-1,j,n+1}-\frac{r_y}{2}T_{i,j-1,n+1}\\&-\frac{r_x}{2}T_{i+1,j,n+1}-\frac{r_y}{2}T_{i,j+1,n+1}\\&=\left(1-r_x-r_y\right)T_{i,j,n+1}+\frac{r_x}{2}T_{i-1,j,n+1}+\frac{r_y}{2}T_{i,j-1,n+1}\\&+\frac{r_x}{2}T_{i+1,j,n+1}+\frac{r_y}{2}T_{i,j+1,n+1}\ ,\end{aligned} \tag{10}$$

where

$$r_x=\frac{\Delta t_h}{\left(\Delta x\right)^2}\ , \tag{11a}$$

$$r_y=\frac{\Delta t_h}{\left(\Delta y\right)^2}\ . \tag{11b}$$

$$\begin{aligned}&(-r_xD^+ +\eta_xA_1)C_{i-1,j,n+1}\\&+(2+\left(2r_x+2r_y\right)D^+ -\Delta tB)C_{i,j,n+1}\\&+(-r_xD^+ -\eta_xA_1)C_{i+1,j,n+1}+(-r_yD^+ +\eta_yA_2)C_{i,j-1,n+1}\\&+(-r_yD^+ -\eta_yA_2)C_{i,j+1,n+1}\\&=(r_xD^+ -\eta_xA_1)C_{i-1,j,n}\\&+(2-\left(2r_x+2r_y\right)D^+ +\Delta tB)C_{i,j,n}\\&+(r_xD^+ +\eta_xA_1)C_{i+1,j,n}+(r_yD^+ -\eta_yA_2)C_{i,j-1,n}\\&+(r_yD^+ +\eta_yA_2)C_{i,j+1,n}\ ,\end{aligned} \tag{12}$$

where

$$r_x=\frac{\Delta t_C}{\left(\Delta x\right)^2}\ , \tag{13a}$$

$$r_y=\frac{\Delta t_C}{\left(\Delta y\right)^2}\ , \tag{13b}$$

$$\eta_x=\frac{\Delta t_C}{2\Delta x}\ , \tag{13c}$$

$$\eta_y=\frac{\Delta t_C}{2\Delta y}\ , \tag{13d}$$

$$A_1=\alpha_1\frac{\partial D^+}{\partial x^+}-\frac{K_1D^+}{T}\frac{\partial\sigma_p}{\partial x^+}\ , \tag{13e}$$

$$A_2=\alpha_1\frac{\partial D^+}{\partial y^+}-\frac{K_1D^+}{T}\frac{\partial\sigma_p}{\partial y^+}\ , \tag{13f}$$

$$K_1=\alpha_2\frac{\Delta V}{R}\ , \tag{13g}$$

$$K_2=\alpha_3\frac{\Delta V}{R}\ , \tag{13h}$$

$$\begin{aligned}B=-\frac{1}{t_C}\Bigg\{&K_1\left(\frac{\partial D^+}{\partial x^+}\frac{\partial\sigma_p}{\partial x^+}+\frac{\partial D^+}{\partial y^+}\frac{\partial\sigma_p}{\partial y^+}\right)\\&-\frac{K_2D^+}{T}\left(\frac{\partial T}{\partial x^+}\frac{\partial\sigma_p}{\partial x^+}+\frac{\partial T}{\partial y^+}\frac{\partial\sigma_p}{\partial y^+}\right)\\&+K_2D^+\left(\frac{\partial^2\sigma_p}{\partial x^{2+}}+\frac{\partial^2\sigma_p}{\partial y^{2+}}\right)\Bigg\}\ .\end{aligned} \tag{13i}$$

Eqn. (10) and eqn. (12) were determined according to the boundary conditions. Then, in order to solve the difference equation, SOR and SUR method was used for eqn. (10) and eqn. (12) respectively. The general equations of SOR and SUR method were given by eqn. (14) and eqn. (15) [9,10].

$$\left[\quad K_{ij}\quad\right]\left\{X_i\right\}=\left\{f_i\right\}\ , \tag{14}$$

$$\begin{aligned}X_i^{(m+1)}=X_i^{(m)}+\beta\Bigg\{&-X_i^{(m)}\\&+K_{ij}^{-1}\left(f_i-\sum_{n=1}^{i-1}K_{ij}X_i^{(m+1)}-\sum_{j=i+1}^{n}K_{ij}X_j^{(m)}\right)\Bigg\},\end{aligned} \tag{15}$$

where, K_{ij} is coefficient matrix, x_i is unknown term, f_i is known term, β is relaxation coefficient and m is step of convergence calculation. Usually, for SOR method, β is taken as $1<\beta<2$. However, since the basic equation includes the first derivative term of hydrogen concentration such as eqn. (5) which leads to unstable convergence, we adopted the method of SUR (Successive-Under-Relaxation) ($0<\beta<1$) for eqn. (15) [10, 22]. To ensure not only mathematical stability but also a physically correct numerical solution, even the Crank-Nicolson method sometimes has limitations on the time and distance increment, Δt^+ and Δr^+ [9,10]. In order to perform accurate numerical analysis, it is necessary to satisfy the condition as shown in eqn. (16) [9,10].

$$\lambda=\frac{\Delta t^+}{\left(\Delta r^+\right)^2}\le\lambda_c(=0.4) \tag{16}$$

.

The hydrogen diffusion and concentration analysis was conducted by FDM. However, various stress components obtained by stress analysis were calculated as the node values. Therefore, these values are necessary to be interpolated from value at each node point for FEM analysis to that at each grid point for FDM analysis. Detailed descriptions of interpolation method were written in previous studies which carried out similar analytical method [9, 11].

Analytical results

Heat transfer analysis

Results of heat transfer analysis are shown in **Fig. 6**. In **Fig. 6**, temperature obtained by this analysis was found to transfer uniformly from WM. This analytical results are considered to be reasonable.

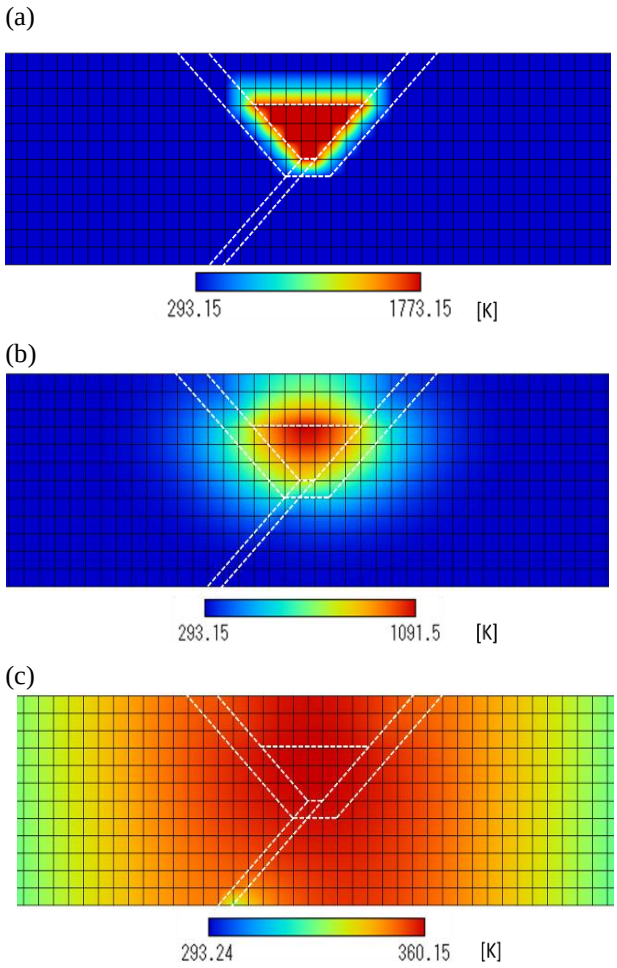

Fig. 6. Time sequential change of 2D temperature distributions. (a) 0step, (b) 10step (0.8sec), (c) 200step (15.6sec)

Hydrogen diffusion and concentration behaviors

Two-dimensional hydrogen concentration distributions are shown in **Fig. 7**. In **Fig. 7**, it was found that hydrogen diffuse from WM to BM through HAZ, and concentrate at the position of blunt angle side of weld groove bottom. The result of y-grooved weld cracking test is shown in **Fig. 8** [23]. Weld cracking also occurred from the position of blunt angle side of weld groove bottom. Therefore, the analytical result obtained by this study well predicted the experimental result. Time sequential change of hydrogen concentration at (x, y) = (62,6) is shown in **Fig. 9**. Where (x, y) = (62,6) corresponds to the position of blunt angle side of weld groove bottom. In **Fig. 9**, however hydrogen concentration initially decreased, after that hydrogen concentration increased with increase in time.

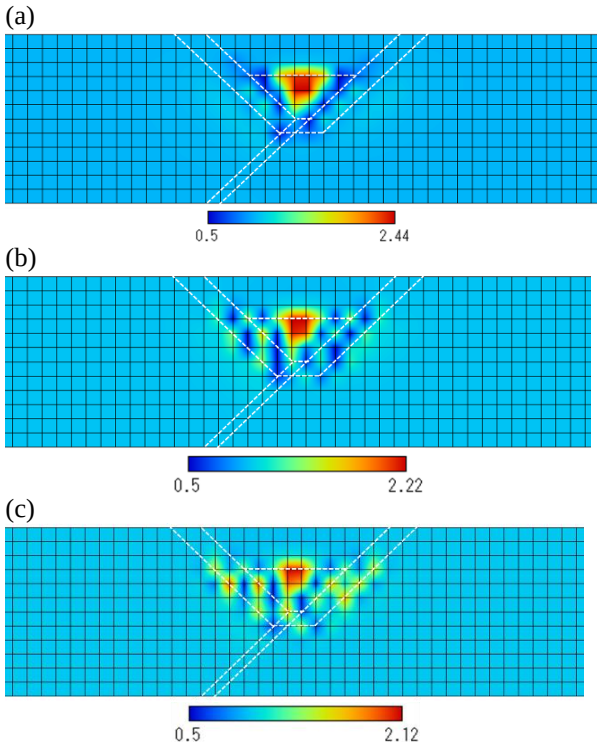

Fig. 7. Time sequential change of 2D hydrogen concentration distributions. (a) 2,000step (156sec), (b) 10,000step (780sec), (c) 18,000step (1403sec)

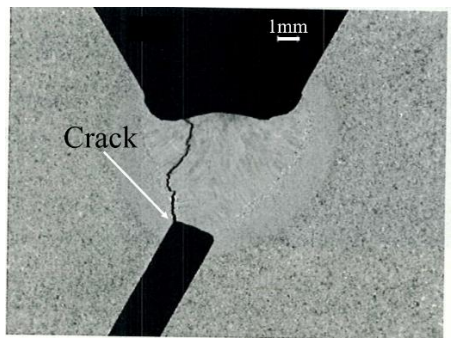

Fig. 8. Experimental result of y-grooved weld cracking test [23].

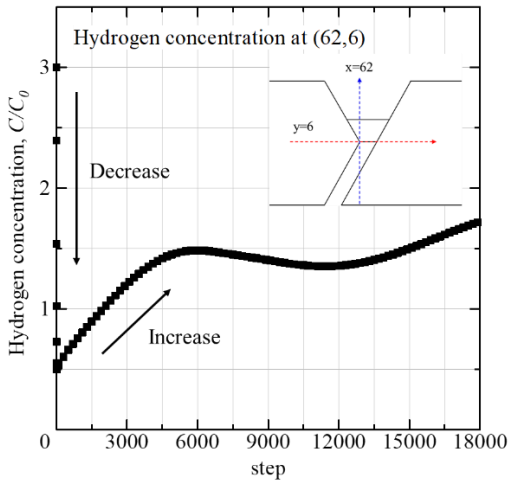

Fig. 9. Time sequential change of hydrogen concentration at (x,y)=(62,6).

Stress analysis

Two-dimensional hydrostatic stress distribution and time sequential change of hydrostatic stress at (x, y) = (62,6) are shown in **Fig. 10** and **Fig. 11**, respectively. From these results, hydrostatic stress increased with increase in time. And, in **Fig. 11**, hydrostatic stress was found to take the local maximum value at the position of blunt angle side of weld groove bottom. This site was found to well correspond with that of hydrogen local concentration. That is, it was shown that hydrogen concentrate at the position of the local maximum value of hydrostatic stress. These results showed that prediction of hydrogen induced cracking caused by hydrogen concentration during cooling process of welding becomes possible using this method of analysis.

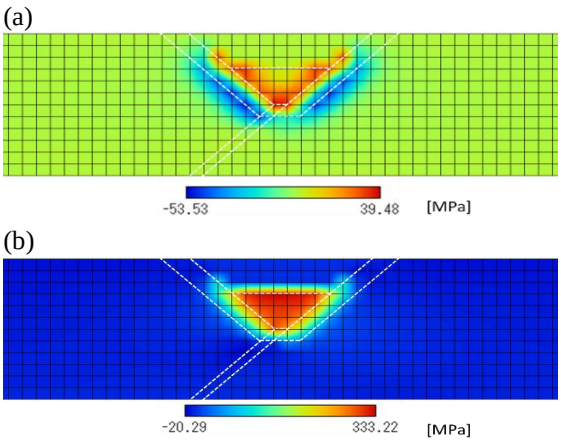

Fig. 10. 2D hydrostatic stress distributions.
(a)1 step (0.08sec), (b) 18,000step (1403sec)

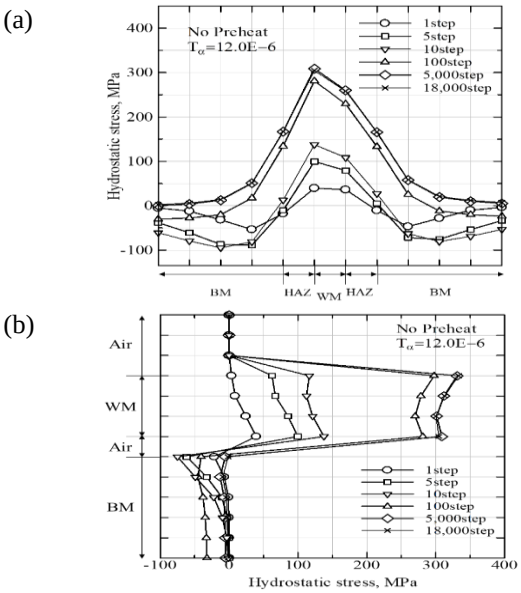

Fig. 11. Time sequential change of hydrostatic stress distribution at (a) y=6, (b) x=62.

Conclusion

By conducting the coupled analysis of heat transfer – thermal stress – hydrogen diffusion for the model of y-grooved weld joint, following results were obtained.

1) Hydrogen was found to diffuse from WM to BM through HAZ, and concentrate at the position of blunt angle side of weld groove bottom.
2) Hydrostatic stress showed the local maximum value at the position of blunt angle side of weld groove bottom. This site was found to well correspond with that of hydrogen local concentration. That is, it was shown that hydrogen concentrates at the position of the local maximum value of hydrostatic stress gradient.
3) These results showed that prediction of hydrogen induced cracking caused by hydrogen concentration during cooling process of welding becomes possible using this method of analysis.

Acknowledgements

This work was supported by Council for Science, Technology and Innovation(CSTI), Cross-ministerial Strategic Innovation Promotion Program (SIP), "Structural Materials for Innovation S" (Funding agency: JST).

Author's contributions

Authors have no competing financial interests.

References

1. N. Yurioka and T. Kasuya, *Quarterly Journal of Japan Welding Society*, **1995**, 13, 3, 347-357.
2. Morlet, J. G., Johnson, H. H. and Troiano, A. R., *Journal of Iron and Steel Institute*, **1958**, 189, 5, 37-44.
3. Oriani, R. A., *NACE-5*, **1973**, 351-358.
4. Liu, H. W., Trans ASME, J. bas. Engng, 92 (1970) 633.
5. T. Ogura and S. Karashima, *Jpn Inst. Metal*, **1971**, 35, 292 (in Japanese).
6. Van Leewen, H. P., *Corrosion*, **1975**, 31, 2, 42-50.
7. M. Iino, *Engineering. Fracture Mechanics*, **1978**, 10,1, 1-13.
8. P. Sofronis, R. M. McMeeking, *Journal of the Mechanics and Physics of Solids*, **1989**, 37, 3, 17-350.
9. A. T. Yokobori, Jr., T. Ohmi, T. Murakawa, T. Nemoto, T. Uesugi and R. Sugiura, *Strength, Fracture and Complexity*, **2011**, 7, 2, 215-233.
10. A.T. Yokobori, Jr., T. Nemoto, K. Satoh and T. Yamada, *Engineering Fracture Mechanics*, **1996**, 55, 1, 47-60.
11. T. Ohmi, A. T. Yokobori, Jr. and K. Takei, *Defect and Diffusion Forum*, **2012**, 326-328, 626-631.
12. A.T. Yokobori, Jr., K. Abe, H. Tsukidate, T. Ohmi and R. Sugiura, H. Ishikawa, *Materials at High Temperatures*, **2011**, 28, 2, 126-136.
13. A. T. Yokobori, Jr., T. Ohmi, G. Ozeki, T. Kasuya, N. Ishikawa, S. Minamoto and M. Enoki, *Proc. of ICF14*, **2017**, edited by E. E. Gdoutos.
14. G. Ozeki, A. T. Yokobori,Jr., T. Ohmi, T. Kasuya, N. Ishikawa, S. Minamoto and M. Enoki, *Proc. of the ASME 2018 Pressure Vessels and Piping Conference*, **2018**, PVP2018-84178 (in press).
15. JIS Z 3158, Method of y-groove weld cracking test, **2016**.
16. Y. Mikami, N. Kawabe, N. Ishikawa and M. Mochizuki, *Quarterly Journal of the Japan Welding Society*, **2016**, 34, 2, 67-80 (in Japanese).
17. K. Satoh, T. Terasaki and Y. Yamashita, *J. of the Japan Welding Society*, **1979**, 48, 7, 504-509 (in Japanese).
18. T. Kasuya, Y. Hashiba, H. Inoue, S. Nakamura, T. Takai, *Welding in the world*, **2013**, 57, 4, 581.
19. Y. Yamada:, Sosei – Nendansei; Baifu-kan Pub:Japan, **1980**, p. 180-219, (in Japanese).
20. T. Kasuya, N. Yurioka, *Welding Journal*, **1993**, 72, 2, 107.
21. A.T. Yokobori Jr. and T. Ohmi, *Strength, Fracture and Complexity*, **2014**, 8, 2, 117-124.
22. S.V. Patankar, Numerical heat transfer and fluid flow; Y. Mizutani and M. Katsuki (Trans.); Morikita Pub. Japan **1985**, p. 70, (in Japanese).
23. T. Kasuya, SIP meeting at the University of Tokyo, April, 2018.

